



Interaction of silver nanoparticle and commonly used anti-inflammatory drug within a poly(amino acid) derivative fibrous mesh

Dóra Barczikai^a, Viktória Kacsari^a, Judit Domokos^b, Dóra Szabó^b, Angela Jedlovszky-Hajdu^{a,*}

^a Semmelweis University, Department of Biophysics and Radiation Biology, Laboratory of Nanochemistry, Nagyvárad tér 4, Budapest, Hungary

^b Semmelweis University, Institute of Medical Microbiology, Nagyvárad tér 4, Budapest, Hungary

ARTICLE INFO

Article history:

Received 29 June 2020

Received in revised form 2 September 2020

Accepted 11 October 2020

Available online 18 October 2020

Keywords:

Nanocomposite
Nanoparticles
Electrospinning
Antibacterial study
Drug release
Paracetamol
Wound dressing

ABSTRACT

In recent decades, wound dressings have evolved from the simple gauze to sophisticated, carefully designed functional materials which can enhance wound healing and eliminate bacterial infections endangering the wounded area. With an increasing number of multidrug-resistant strains, bacterial overgrowth of the injured area poses a serious risk that can lead to severe conditions. Nanoparticles can exhibit remarkable antibacterial properties thus incorporating them into biocompatible matrices, effective antibacterial wound dressings can be fabricated. Utilizing electrospinning, nanoparticles could be easily incorporated into fibrous polymer meshes. Next to nanoparticles, electrospinning allows the simultaneous encapsulation of small molecules as well, resulting in complex nanocomposite meshes exhibiting antibacterial and anti-inflammatory and/or analgesic properties. In the manuscript, we present a one-pot method for the synthesis of silver nanoparticles (AgNP) in the presence of polysuccinimide (PSI) and a small molecule drug (paracetamol), followed by the fabrication of an antibacterial wound dressing system. Thorough characterization of both the AgNP-containing colloidal system and the meshes were performed. Results reveal the stabilizing effect of PSI and paracetamol enhancing the formation of a monodisperse colloidal system. Mechanical studies confirm the reinforcing effect of silver-nanoparticles, and antibacterial evaluation proves the applicability of the meshes. Drug-release measurement shows prolonged three-step release kinetics.

© 2020 The Authors. Published by Elsevier B.V. This is an open access article under the CC BY license (<http://creativecommons.org/licenses/by/4.0/>).

1. Introduction

Wound healing is defined as the process where damaged or lost tissues are either regenerated or replaced. This process involves a complex sequence of events and mechanisms composed of neural feedbacks, chemical, and molecular interactions as well as cellular movement, proliferation, and differentiation. Aberrations in wound healing, result due to either local (e.g. moisture, oedema, infection) or generalized (e.g. diabetes, smoking, immunosuppression) conditions [1]. These factors can delay or entirely prevent proper wound healing consequently resulting in chronic conditions. In order to prevent the negative effect of these factors and enhance the healing process, medical and scientific research has been increasingly focusing on the functionalization and optimization of wound dressings [2–4].

Wound dressings have evolved to sophisticated materials with intricate structures and specialized components, designed specifically to enhance and promote faster wound healing rates. While simple gauze dressings are still widely used, wound dressings are now not exclusively composed of textiles. The research focus is now turning to advanced

materials, for example, films, hydrogels, foams, and nanofibers with an emphasized objective on the prevention of bacterial infection, since such an event can seriously delay the healing process and poses as a major risk towards severe clinical conditions [3–7]. Each with its own advantages and disadvantages, these modern materials are employed as they are structurally designed to support the healing, absorb excess wound exudate while preventing dehydration of the wounded area and they can be combined with pharmaceutical agents providing analgesia, and most importantly antibacterial agents preventing infections [5,8,9].

While typically bacterial flora found on the skin poses no risk to a patient, as the balance of the skin is disrupted due to chronic wounds or immunocompromised conditions, even representatives of normal bacterial flora can lead to pathological conditions [5]. *Staphylococcus epidermidis* is part of healthy skin microbiota but is also known as one of the leading causes of nosocomial infections and is rather hard to eradicate with conventional antibiotics due to its biofilm-forming characteristics [10–12]. Another bacterial strain typically acquired as a nosocomial infection, *Pseudomonas aeruginosa* plays a crucial part in impaired wound healing and exhibits extraordinary resistance towards a wide range of antibiotics [13]. To overcome the widespread antibiotic resistance of various pathogens, several strategies have

* Corresponding author at: Nagyvárad tér 4, 1089 Budapest, Hungary.

E-mail address: hajdu.angela@med.semmelweis-univ.hu (A. Jedlovszky-Hajdu).

been continuously proposed and examined. These tactics include antibacterial polymers, essential oils, and other natural antibiotics such as honey, antimicrobial peptides, phage therapy, and nanoparticles [5,13,14]. Nanoparticles (NPs) are particularly effective against bacterial infections, and they seem to be a promising candidate to replace antibiotics against multidrug-resistant strains. According to various studies, three mechanisms are proposed for the antibacterial action of NPs: a. release of metal ions b. oxidative stress c. non-oxidative mechanisms. Due to these three modes of action, NPs can effectively penetrate the bacterial membrane, disrupt biofilm formation, generate reactive oxygen species, or even destabilize ribosomes [12,13,15].

One popular compound investigated regarding wound dressing applications is silver, as it exhibits exceptional antibacterial properties. In particular silver nanoparticles (AgNP) have been investigated and their positive results have been demonstrated several times yet, some controversy still surrounds the subject [16]. While overall effective, modifications to augment their effect are still possible. Their mechanism of action involves damaging the bacterial cell membrane as well as the bacterial DNA [17]. Recently the correlation between the nanoparticle size and surface area/volume ratio to antibacterial effect has been examined. AgNP distribution and size directly affect the total "antibacterial surface" and thus the overall silver ion release and antibacterial efficacy. For a wound dressing material to be a proper template for silver nanoparticles an essential prerequisite is to facilitate the silver ion release. In this regard, nanofibers – possessing a high specific surface area– can provide an excellent carrier for silver nanoparticles.

Nanofibers have been widely utilized in regenerative medicine and tissue engineering as they possess several advantageous features [18,19]. Undeniably, besides their chemical compositions, a wound dressing's physical structure can greatly impact the wound healing process. Nanofibers have a microstructure resembling the extracellular matrix innately found around almost every cell in the human body. Nanofibrous meshes are typically composed of either naturally occurring (e.g. chitosan, alginate, hyaluronic acid) or synthetic (poly(ϵ -caprolactone), poly(lactic acid), poly(vinyl alcohol)) polymers [20–22]. Even without antibacterial properties nanofibrous meshes have some interesting properties that can be useful for wound care such as absorbing wound exudate, the release of analgesic pharmaceutical compounds, promoting haemostasis phase due to their high surface area and also their structure leads to semi-permeability which facilitates the respiration of the cells [23]. However, since bacterial infection is one of the leading causes of impaired wound healing, without antibacterial efficacy nanofibrous meshes couldn't eliminate the risk of such an infection and their use in woundcare is rather limited.

Nanofibrous meshes containing silver nanoparticles have been previously investigated yet, to our knowledge AgNPs have not been combined with poly(succinimide) (PSI) based nanofibrous systems.

Poly(succinimide) is a polymer produced by the thermal polycondensation of L-Aspartic acid. It is a water-insoluble polymer that hydrolyses in even mild alkaline environment, such as physiological pH. Additionally, PSI is easily modified as it is prone to react with nucleophiles under mild conditions, resulting in water-soluble poly(aspartic acid) (PASP) and its derivatives. These features coupled with its biocompatible and biodegradable nature, make it a promising polymer for tissue engineering, cell cultivation, and other biotechnological applications. Utilizing PSI, hydrogels, nanogels, films, fibrous hydrogels, and also non-woven fibrous meshes can be prepared [24–27].

Electrospinning is one of several methods (e.g. wet-spinning, dry-spinning, etc.) that is currently used to produce non-woven nanofibrous membranes. Using a high voltage, provided by a power supply, nanofibers can be fabricated from polymer solutions as they are pushed through a needle. This method is quite prevalent as it is straightforward but also provides numerous possibilities for modification and adjustments making it probably the most versatile and cost-effective out of all the spinning methods [28–30].

In this manuscript, we are demonstrating how AgNPs as well as pharmaceutical agents can be electrospun after a one-pot synthesis method. The pharmaceutical agent of choice was paracetamol (APAP), perhaps the most frequently used Non-Steroidal Anti-Inflammatory Drug (NSAID). Our aim, by pairing paracetamol with AgNPs is to assess the effect of a small-molecular drug on AgNP and how it could potentially enhance or decrease the antibacterial effect of PSI based membranes. Furthermore, PSI being a highly biocompatible polymer the objective is to produce a functionalized biocompatible and biodegradable wound dressing.

In the following manuscript, we present the synthesis and characterization of AgNPs and the fabrication and characterization of AgNP and paracetamol containing PSI electrospun meshes. Silver nanoparticles are known to be effective against biofilm-forming and multidrug-resistant bacteria strains, therefore they are an excellent component to incorporate in modern functional wound dressings. Since the properties of these aforementioned particles depend on their colloidal properties, our aim was to develop an efficient one-pot method for the synthesis of silver nanoparticles with tuneable properties in the presence of a polymer (polysuccinimide, PSI) and a small-molecule drug as well.

This work incorporates both physical (Dynamic Light Scattering, Scanning Electron Microscopy) and mechanical characterization of the meshes but also the antibacterial effect of AgNPs on four different bacterial strains (*E. coli*, *P. aeruginosa*, *B. subtilis*, *S. epidermidis*) as well as the drug-release profile of the paracetamol and finally a method was proposed to compare the antibacterial effect of meshes with different composition.

2. Materials and methods

2.1. Materials

L-aspartic acid (reagent grade, $\geq 98\%$, Amresco), orthophosphoric acid ($\geq 99\%$, Sigma Aldrich), N,N-dimethylformamide (DMF, anhydrous, $\geq 99.94\%$, Reanal), chromosulfuric acid (Sigma-Aldrich), silver-perchlorate (AgClO_4 , Sigma-Aldrich), paracetamol (APAP, puriss, 98,0%, Alfa Aesar), phosphate buffered saline tablet (PBS, Sigma-Aldrich), Mueller-Hinton agar (Biolab Zrt.), *E. coli* ATCC 25922, *S. epidermidis* ATCC 14990, *P. aeruginosa* ATCC 27853, *B. subtilis* ATCC 6633.

All reagents and solvents were used without further purification.

2.2. Synthesis of polysuccinimide

Polysuccinimide (PSI) was prepared by thermal polycondensation of L-aspartic acid in the presence of orthophosphoric acid. According to a previously reported method [31], L-aspartic acid and orthophosphoric acid were mixed at a 1:1 weight ratio in a rotating flask and the mixture was gradually heated up to 180 °C while the pressure was gradually reduced to 3 mbar using a rotary evaporator. The flask was constantly rotated at 130 rpm for 8 h. The resulting polymer was subsequently dissolved in 170 ml dimethylformamide, then precipitated in deionized water and washed several times until a neutral pH was reached. Finally, the resulted PSI powder was dried at 40 °C until changes in mass were not detectable. The polymer was stored in close containers at room temperature.

2.3. Synthesis of silver nanoparticles

For the synthesis of silver nanoparticles, a one-pot method was developed based on a previously reported synthesis method [32]. First, 1 g of PSI was dissolved in 4 g of DMF to reach a polymer-concentration of 20 w/w%. When the dissolution was complete, the solution was saturated with argon after which 0.1 g of AgClO_4 was added to the mixture under the established inert atmosphere. Four different

samples were prepared according to the concentration of paracetamol. Table 1 summarizes the parameters of the prepared samples. In all cases, reaction mixtures were kept in closed vessels under an inert atmosphere and stirred for 72 h at 300 rpm and 60 °C (Radleys reactor, IKA RCT Basic magnetic stirrer).

Samples were always stored under an inert atmosphere until further processing.

Important to mention is that, before every synthesis, every glassware was cleaned using concentrated chromosulfuric acid and thoroughly washed with ultrapure water (Conductivity <0.1 µS/cm) to avoid cross-contamination.

2.4. Dynamic Light Scattering

After the 72-hour reaction time, the size and polydispersity of the silver nanoparticles within the PSI/DMF dispersion was evaluated using a Malvern Nanosizer S instrument equipped with a 4 mW He-Ne laser ($\lambda = 632.8$ nm). Samples were diluted with pure DMF. The performed dilution was proportionate to the paracetamol content. In each case, samples were diluted to optimize the count rate and the gyration coefficient. Approximately 200 µl of the diluted sample was poured into a disposable cuvette suitable for organic solvents. Details of the measurements were the following: 3 measurements; the number of runs: 15 (each 15 s); backscattering method; temperature: 25 °C. A general-purpose analysis model was utilized for data processing then the Stokes-Einstein equation was used for the calculation of size.

2.5. Electrospinning

For the fabrication of silver-nanoparticle (AgNP) containing PSI meshes (denoted as AgNP/PSI) and for the fabrication of meshes containing both silver-nanoparticle and paracetamol (denoted as AgNP/APAP/PSI) a two-needle electrospinning setup was used. The setup comprised of two 5 ml Luer-slip syringes (Chirana, Slovakia) with 18G metal needles (Becton Dickinson, USA), two single-syringe infusion pumps (KDS100, KD Scientific, USA) placed opposite to each other on the two sides of the rotating collector as it is shown on Fig. 1, and high voltage DC supplies (73030P series, Genvolt, UK) and a slowly rotating cylindrical collector (RPM = 50, d = 12 cm).

The silver nanoparticle and polymer containing dispersions were transferred to syringes to which metal needles were attached. Loaded syringes were then secured to the infusion pumps. Positive electrodes were attached to the tips of the metal needles while the negative electrodes were clamped to the rotating collector. The electric potential was provided by the high voltage DC supplies.

Meshes were fabricated within a week after the synthesis at room temperature ($T = 25 \pm 2$ °C) and at relatively low humidity (Humidity = $22 \pm 3\%$). The electrospinning parameters of all the fabricated samples are summarized in Table 2.

In the Results and discussion section, $c_{\text{paracetamol}}$ is always given as **paracetamol content mg/5 g** where 5 g always refers to the amount of 20 w/w% PSI/DMF polymer solution.

In the case of the sample designated as 0 + 10, 10 mg of paracetamol was added to a batch of 0 mg paracetamol/5 g polymer solution after the 72-hour reaction and right before electrospinning to yield a physical mixture. After the addition of paracetamol, these samples were stirred for only 15 min at room temperature to achieve a homogeneous distribution in the highly viscous colloidal system.

2.6. Scanning Electron Microscopy

To investigate the microstructure of the meshes, Scanning Electron Microscopy was utilized. Images were taken with a JSM 6380LA scanning electron microscope (JEOL, Japan). Samples were secured on an adaptor with double-sided carbon tape and then coated with a thin layer of gold using a JFC-1200 Sputter Coating System (JEOL, Japan) to ensure the required conductivity for the measurement. The applied voltage was 15 kV and the working distance was 10 cm. Pictures were obtained at a 1000×, 5000× and 10,000× magnification. Fibre diameters were determined using Fiji ImageJ software from at least 50 fibres and a non-parametric one-way ANOVA analysis (Kruskal-Wallis test) was performed on fibre diameter values to decide which samples have significantly different diameter ($p < 0.05$). Statistical evaluation was performed using STATISTICA 10 software.

2.7. Mechanical testing

The loading capacity of the meshes was evaluated with an Instron 4952 unidirectional mechanical tester (50 N measuring cell). As summarized in Table 2, six different meshes were fabricated and examined. 1.5×6 cm test specimens ($N = 5$) were cut from each electrospun mesh parallel to the rotation of the collector as indicated in Fig. 2/a. Samples were placed between the grips of Instron mechanical tester symmetrically on both ends (Fig. 2/b). Measurements were performed at a 1 mm/min pulling speed until the complete tear of test specimens. The exact size and mass of the test specimens were measured and recorded.

The specific maximum load was attained by dividing the maximum sustained load from the recorded force-deformation curve by the surface mass density (mass/area) to obtain specific maximum load:

$$\text{Specific maximum load} \left(N * \frac{m^2}{g} \right) = \frac{\text{Maximum load (N)}}{\frac{\text{mass (g)}}{\text{Area (m}^2\text{)}}}$$

A non-parametric one-way ANOVA analysis (Kruskal-Wallis test) was performed on specific maximum load values to determine whether samples significantly differ from each other ($p < 0.05$). Statistical evaluation was performed using STATISTICA 10 software.

Table 1
Parameters of reaction mixtures.

C_{AgClO_4} (g/5 g 20 w/w% PSI solution)	$C_{\text{paracetamol}}$ (g/5 g 20 w/w% PSI solution)	Reaction parameters			Paracetamol-addition
		T [°C]	V_{stirring} [rpm]	t [h]	
0.1	0	60	300	72	–
0.1	5	60	300	72	Before AgClO ₄
0.1	10	60	300	72	Before AgClO ₄
0.1	50	60	300	72	Before AgClO ₄

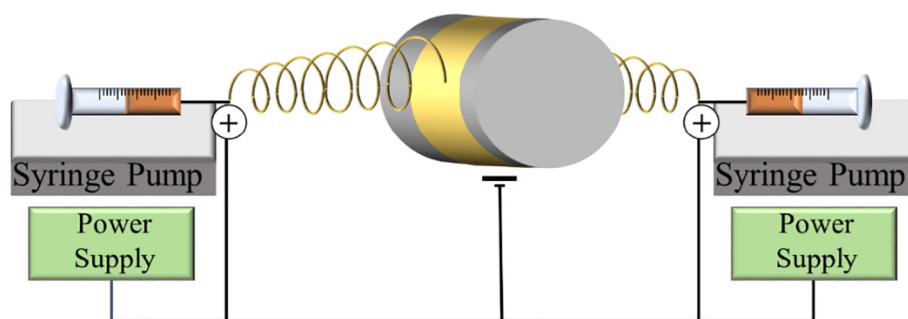


Fig. 1. Two-needle electrospinning setup for the fabrication of nanofibrous meshes.

2.8. Evaluation of antibacterial properties

Antibacterial activity was evaluated using the standardized Kirby-Bauer disc diffusion method. Four ATCC (American Type Culture Collection) bacterial strains were used, namely: *E. coli* (Gram-negative), *P. aeruginosa* (Gram-negative), *B. subtilis* (Gram-positive) and *S. epidermidis* (Gram-positive).

Bacteria colonies from each strain were immersed individually into 5 ml of saline and then the suspensions were diluted to reach a 0.5 McFairland turbidity using a DEN-1 Benchtop Densitometer (Grant Instruments). A sterile swab was then immersed into the bacteria-containing saline after which the Muller-Hinton agar was covered with the bacteria containing solution using the swab.

Before the antibacterial evaluation, membrane discs with a diameter of 6 mm were cut from the meshes ($n = 3$ per mesh and per bacteria strain) and the mass of each disc was measured and recorded. Discs were sterilized at 120 °C for 2 h using a dry heat sterilizer. These sterile discs were placed onto the top of the inoculated Muller-Hinton agar and then the plates were incubated for 24 h at 37 °C. After 24 h, the diameter of the bacteria-free zone (diffusion zone) was measured for each disc.

This evaluation aimed to determine the effect of paracetamol content on the antibacterial properties of silver nanoparticles. Therefore, to evaluate the effect of the silver nanoparticles within the meshes, the antibacterial areas around the test discs were calculated and divided by the silver- content (*Specific antibacterial area*).

$$\text{Specific antibacterial area} \left(\frac{\text{cm}^2}{\text{mg Ag}} \right) = \frac{\left(\frac{d_{\text{zone}}}{2} \right)^2 * 3.14 - \left(\frac{d_{\text{mesh}}}{2} \right)^2 * 3.14}{m_{\text{Ag}}}$$

2.9. Drug-release kinetics

Drug-release kinetics of $C_{\text{paracetamol}} = 10 \text{ mg/5 g PSI solution}$ and $C_{\text{paracetamol}} = 5 \text{ mg/5 g PSI solution}$ meshes were examined with an Agilent 8453 UV-VIS Spectrophotometer. Samples of approximately 0.1 g were gently placed into dialyzing membranes (cut-off =

14 kDa). The dialyzing membranes containing the examined meshes were closed tightly on both ends and immersed into 15 ml of phosphate-buffered saline (PBS, $I = 0.15 \text{ M}$, $\text{pH} = 7.4$) in a glass vessel. Release media were kept at 37 °C while constantly stirred with magnetic bars. At predetermined time intervals, 2 ml of the media was removed and the absorbance values were measured. The removed volume was replaced with fresh PBS and it was followed for 1 week.

3. Results and discussion

3.1. Synthesis of silver nanoparticle in the presence of PSI

Silver nanoparticles were synthesized via a one-pot method based on the reaction of silver salt and DMF. The schematic representation of the whole synthesis procedure can be seen in Fig. 3.

This reaction has been well-documented for years now, however, the addition of a stabilizing agent is required as DMF itself couldn't stabilize the formed nanoparticles. Without a stabilizing agent, aggregation takes place immediately in the solution followed by precipitation which results in macroscopic silver or in simple terms a silver-mirror (a thin silver layer on the side of the glass synthesis chamber). This phenomenon was also observed in our system where silver-perchlorate and DMF were mixed for 72 h at 60 °C. Silver precipitation was noticeably visible on magnetic bars and the glassware.

On the contrary, in the presence of polysuccinimide (PSI), instead of silver-precipitation, a clearly visible colour change was observed.

While the solution initially is transparent yellow (typical colour of a PSI/DMF solution) it turns to dark brown during the synthesis. The presence of paracetamol next to PSI during the reaction results in a dark dun colour, different from the colour of the mixture without paracetamol (sleek dark brown – characteristic of stable colloidal sols). This difference between the samples was most noticeable for the highest paracetamol content (50 mg/5 g polymer solution) (Fig. 4). The colour-change upon increasing paracetamol content is an indirect proof for the growing particle size of the colloidal system. To prove this prediction, DLS measurements were performed.

Table 2
Electrospinning parameters.

Type of the mesh	C_{PSI} (w/w%)	C_{AgClO_4} (g/5 g PSI solution)	$C_{\text{paracetamol}}$ (mg/5 g PSI solution)	Spinning parameters			
				Voltage (kV)	Distance (cm)	Flow rate (ml/h)	Specifications
PSI	20	0	0	15	10	0.8	Slowly rotating collector, 1 needle
AgNP/PSI	20	0.1	0	15	10	0.4	Slowly rotating collector;
AgNP/APAP/PSI	20	0.1	5	12–13	10	0.4–0.5	double-needle setup
	20	0.1	0 + 10	12–13	10	0.4	
	20	0.1	10	12–13	10	0.4	
	20	0.1	50	12	10	0.4	

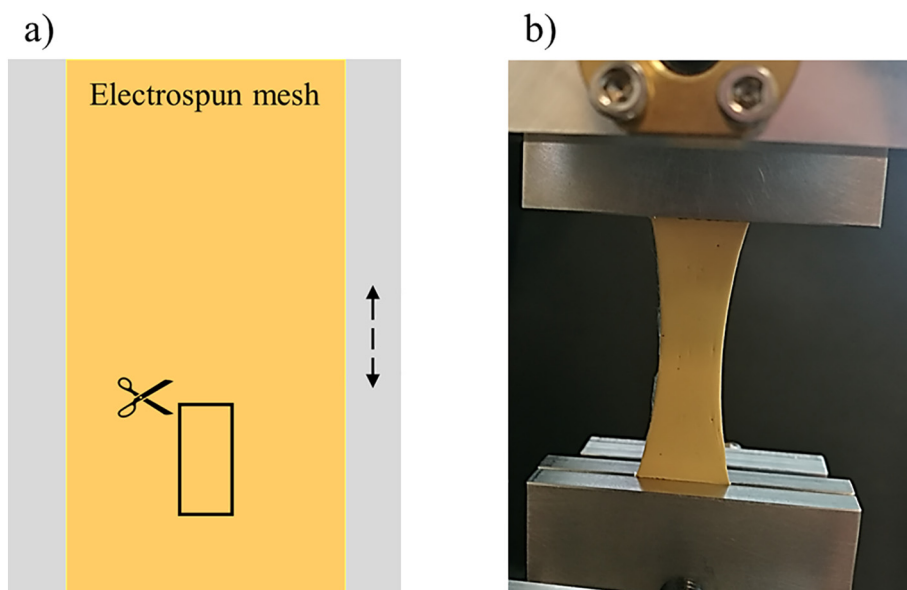


Fig. 2. Sample preparation for mechanical testing: a) box represent test specimen cut from electrospun mesh (arrow indicates rotating direction of cylindrical collector), b) test specimen under load.

Based on previous measurements, reaction mixtures containing 0.1 g silver in 5 g 20 w/w% PSI (without the addition of paracetamol), these colloidal systems retain their aggregative stability for more than 1 month. During 6 weeks no precipitation was observed, evidently indicating that PSI can prevent the aggregation and successfully stabilize the formed nanoparticles within this period of time.

To examine the contribution of paracetamol to this stabilizing effect, reaction mixtures without PSI were also prepared. In this case, silver precipitation was observed on the magnetic bar and on the glass vessel indicating that paracetamol may have a contribution to the stabilization but in itself is not effective enough to prevent precipitation (Fig. S1, Supplementary Information).

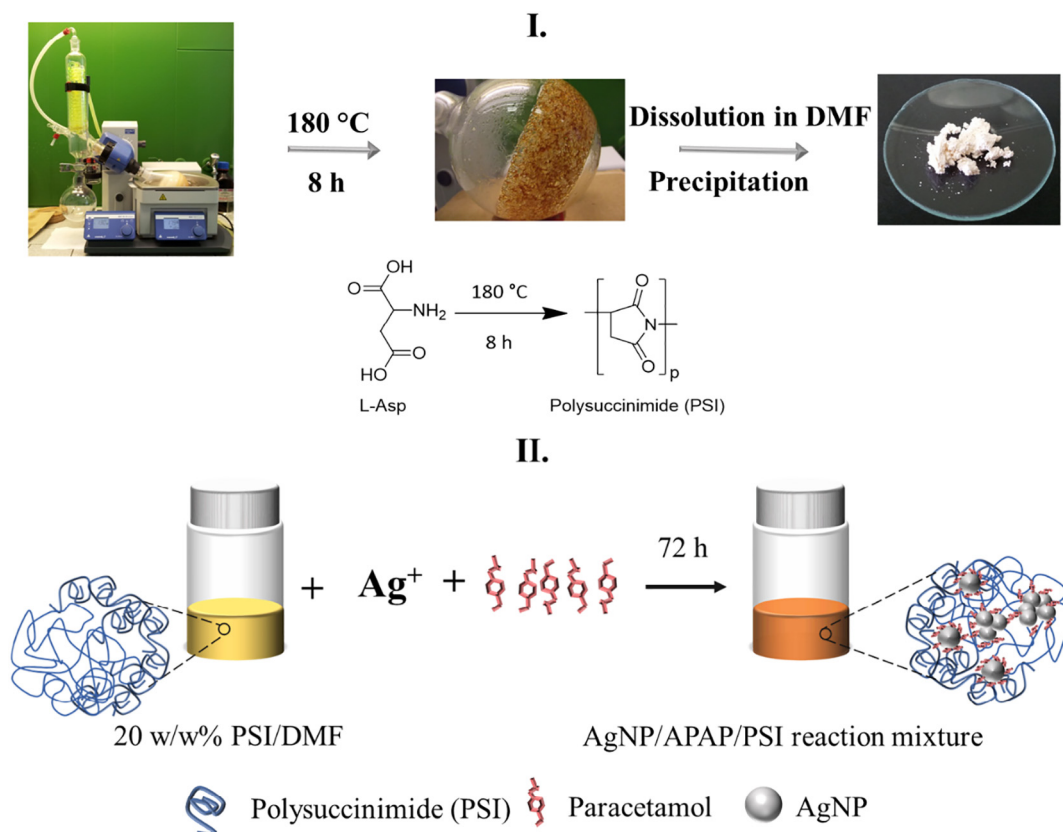


Fig. 3. Schematic representation of PSI synthesis and the following silver-nanoparticle synthesis.

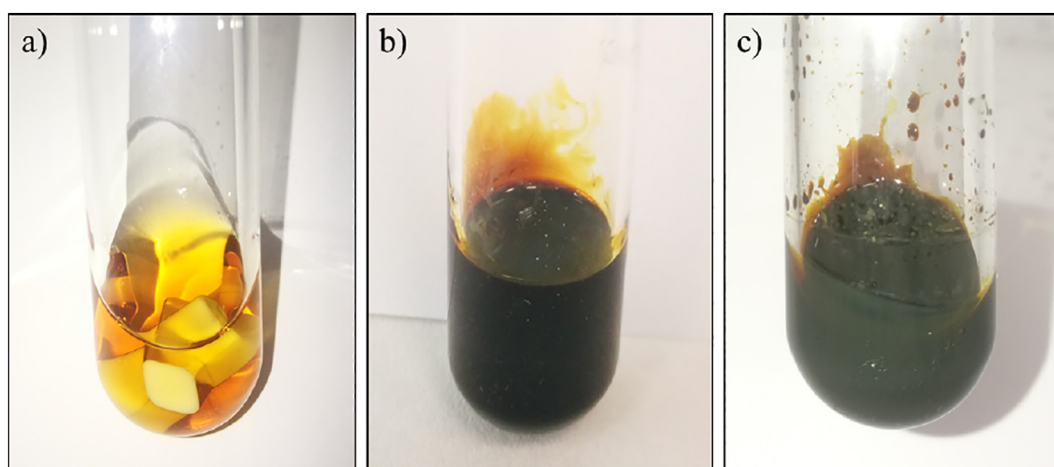


Fig. 4. Colour of the synthesis mixtures: a) PSI/DMF solution b) PSI/DMF and 0.1 g AgClO_4 reaction mixture after 72 h c) PSI/DMF, 0.1 g AgClO_4 and 50 mg paracetamol after 72 h.

3.2. Characterization of silver nanoparticles by Dynamic Light Scattering

Antibacterial properties of silver nanoparticles are known to be strongly dependent on the size of the particles therefore size-determination is a key aspect in designing effective silver nanoparticle-containing matrices. For a thorough characterization, the mean size of the silver nanoparticles was calculated not just based on intensity, but the size and volume distribution as well. The latter two were calculated from intensity distribution using Rayleigh ($d < \lambda_{\text{laser}}/10$) or Mie-theory ($d > \lambda_{\text{laser}}/10$) [33].

Three different weighting methods and four parameters (z-average and intensity-mean, number-mean, volume-mean) can be utilized to gain more precise and comprehensive information about the colloidal system in question. One of the most important and most frequently reported parameters of a colloidal system is Z-average which is an intensity-based attribute determined by a fit to the correlation function. Along with intensity-mean, these two parameters represent the mean size of the nanoparticles that contributes most to the overall scattering thus weighting bigger particles more heavily. On the contrary, number-mean derives from the number of particles without taking into consideration particle size, therefore particles of different sizes are counted having equal numerical value. Therefore, z-average, intensity-mean, and volume-mean are rather sensitive to the presence of aggregates while the number-mean can be used to demonstrate the individual (not aggregated) smaller particles of the system. These four parameters alongside with polydispersity index (PDI) of the colloidal system in question are shown in Fig. 5.

By plotting the polydispersity index (PDI) as a function of the paracetamol content (Fig. 5/a), it can be concluded that paracetamol can reduce the value of PDI from 0.3 to below 0.1 indicating that increasing amount of paracetamol facilitates the formation of a highly monodisperse colloidal system. Compared to the PDI, Z-average (Fig. 5/a), namely the overall average size of the colloidal system, demonstrates an opposing behaviour: initially due to the small amount of paracetamol content the z-average size decreases then as the paracetamol content increases, nanoparticle size increases accordingly. This behaviour and the size of the nanoparticles are rather perplexing to interpret and it requires not only z-average but intensity-, number- and volume-mean as well (Fig. 5/b). The cause of the initial decrease is probably due to paracetamol being able to hinder the aggregation of the nanoparticles in a more effective manner than PSI in itself does. While PSI can prevent the precipitation of silver nanoparticles, it also can not entirely impede particle aggregation indicated by the initial gap between number-mean size and intensity-mean size. The higher value of intensity-mean size (and z-average) suggests the presence of aggregates while the low value of number-mean size demonstrates that the majority of the particles still have an average size of 37 nm. Upon addition of paracetamol, even in a small concentration (5 mg/5 g PSI solution), intensity-, volume- and number-mean values start to approximate each other which implies that an increase in the paracetamol content results in a more well-defined, larger sized but monodisperse colloidal system with narrow size deviations.

To further visualize the effect of paracetamol on the properties of this complex colloidal system, intensity distributions were compared to each other (Fig. 5/c). The intensity-distribution comparison is quite

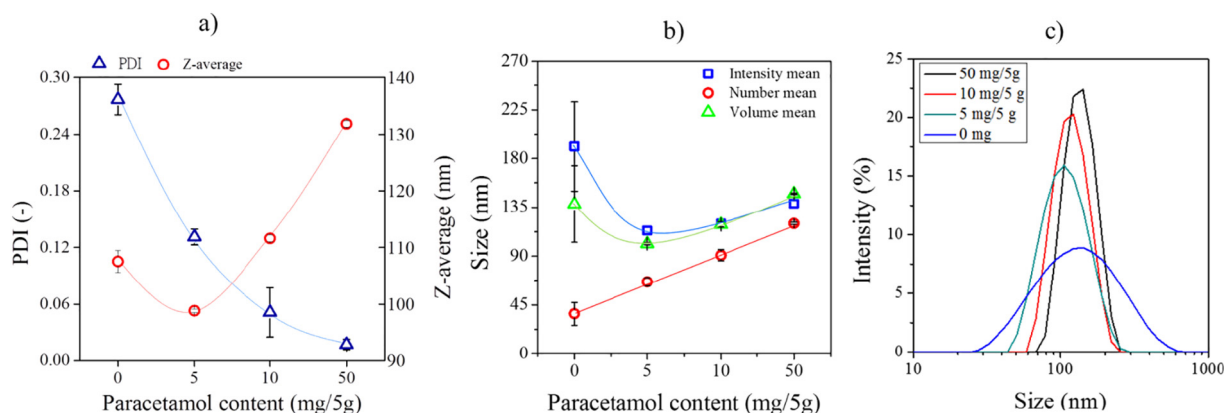


Fig. 5. Effect of paracetamol on properties of silver nanoparticles a) polydispersity index (PDI) and z-average b) particle size and c) intensity-based size distribution.

informative regarding the effect of paracetamol. Increasing paracetamol content results in a narrower size distribution and a higher maximum value indicating that paracetamol facilitates the formation of a highly monodisperse colloidal system.

The results are quite promising since they evidently indicate that PSI in itself can promote the synthesis of a colloidal system with a PDI value no greater than 0.3. Furthermore, by adjusting the quantity of paracetamol the parameters of this silver colloidal system can be altered in accordance with the desired properties. Additionally, the synthesis method seemed to have a satisfying reproducibility (Fig. S2, Supplementary Information).

3.3. Electrospinning

Due to the fact that the reaction mixture doesn't require further purification or processing, electrospinning could be performed right after the 72-hour reaction. Noteworthy mentioning is that, while simple, PSI-only meshes are white, AgNP/PSI and AgNP/APAP/PSI meshes are bright yellows. In some cases, instead of bright yellow colour, a pale beige – white colour was observed (Fig. 6). In these cases, the reaction mixture was analysed with DLS in terms of PDI and particle-size to examine the possible cause of this pale colour. These DLS data showed a rather high polydispersity and noisy raw correlation data (Fig. S3, Supplementary Information) implying that the reduction of silver ions and the consecutive nanoparticle-formation wasn't complete. Therefore, the vibrant yellow colour seems to be a fast, simple, and reliable indicator of the mesh and colloid system quality.

Meshes prepared from 50 mg/5 g paracetamol had a slightly darker colour, but every mesh had the characteristic vibrant yellow colour. No differences could be observed in texture or manageability nor between samples containing different amount of paracetamol, nor between pure PSI and nanoparticle-containing meshes.

Additionally, X-ray Diffraction studies were performed in order to determine the crystallinity of silver nanoparticles and the physical form of the encapsulated paracetamol within the meshes. Further details about the measurements could be found in Supplementary Information. Briefly, the results suggest that the presence of paracetamol enhances the formation of crystalline silver-nanoparticles instead of amorphous form while crystalline paracetamol couldn't be detected in the examined sample (Fig. S4, Supplementary Information)

3.4. Fibre morphology and size distribution assessment by Scanning Electron Microscopy

Scanning Electron Microscopy images confirm that the electrospinning method was successfully optimized for every sample. All

samples have a homogenous, randomly orientated fibrous structure without beads or other artefacts (Fig. 7).

By applying higher magnification, the surface of the fibres can be evaluated more precisely. Fig. 7 shows a higher magnification only of a mesh prepared from 0 mg/5 g paracetamol reaction mixture, of which microstructure is representative and similar to those of the other meshes as well. Higher magnification depicts a randomly orientated structure and a particularly smooth surface without observable clots or beads.

Based on fibre analysis, average fibre diameters were calculated for each type of mesh (Table 3). The average diameter seems to increase in accordance with increasing paracetamol content in case of samples where paracetamol was present during the 72-hour reaction (5, 10, and 50 mg/5 g paracetamol). In case of meshes prepared from 0 + 10 mg/5 g paracetamol mixtures (where paracetamol was added to the 0 mg/5 g mixture right before electrospinning to yield a physical mixture), the diameter is approximately the same as in case of 0 mg/5 g.

To examine whether paracetamol content and/or particle size in the colloidal state have a significant effect on the fibre diameter statistical analysis was performed on fibre diameter values. The statistical results suggest that fibre diameters significantly differ from each other except for 0 (without drug) and 0 + 10 (physical mixture) samples which two samples possess approximately the same average fibre diameter (results concluded in Table S1, Supplementary Information). This implies that a change in the microstructure occurs upon increasing paracetamol content but since 0 + 10 sample has the same diameter as 0 sample, the change is due to an indirect effect of paracetamol and not solely its presence in the reaction mixture. Fibre diameter increases with paracetamol content which is following the change of number mean size of the particles upon growing paracetamol content (Fig. 5/b). Subsequently, this comparison suggests that increasing paracetamol content could have an indirect effect on fibre diameter through altering particle size in the reaction mixture during the 72-hour reaction, and therefore diameter increases in accordance with the number-mean size itself. Since in the case of 0 + 10 mg/5 g sample, paracetamol was only added to the system right before electrospinning, nanoparticle size was the same as for 0 mg/5 g sample, thus fibre diameters of these two compositions stay approximately the same.

When comparing particle sizes in colloidal state (Fig. 5) and fibre diameter (Table 3) it is important to know that the size measured by DLS is not equivalent to particle size inside the mesh. Fig. 8 demonstrates the particle size measured in the colloidal state by DLS and the schematic hypothesised process of electrospinning at a molecular level. DLS measures not only the silver-nanoparticle but also the paracetamol and/or PSI layers being adsorbed to the silver-core. During electrospinning, the polymer chains and silver nanoparticles are aligned and rearranged

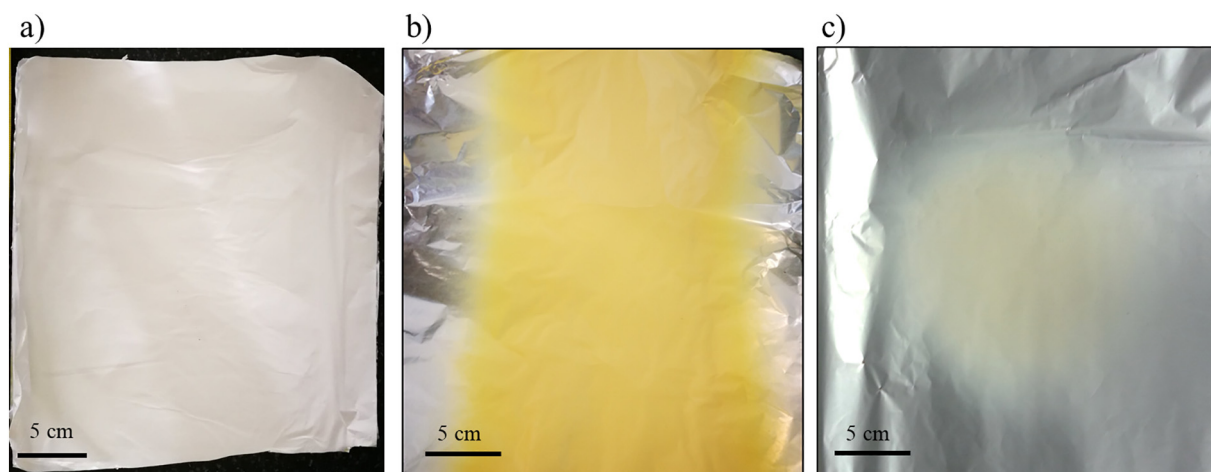


Fig. 6. a) PSI mesh b) characteristic yellow colour of AgNP/APAP/PSI mesh with good quality DLS results c) AgNP/APAP/PSI mesh with poor quality DLS results.

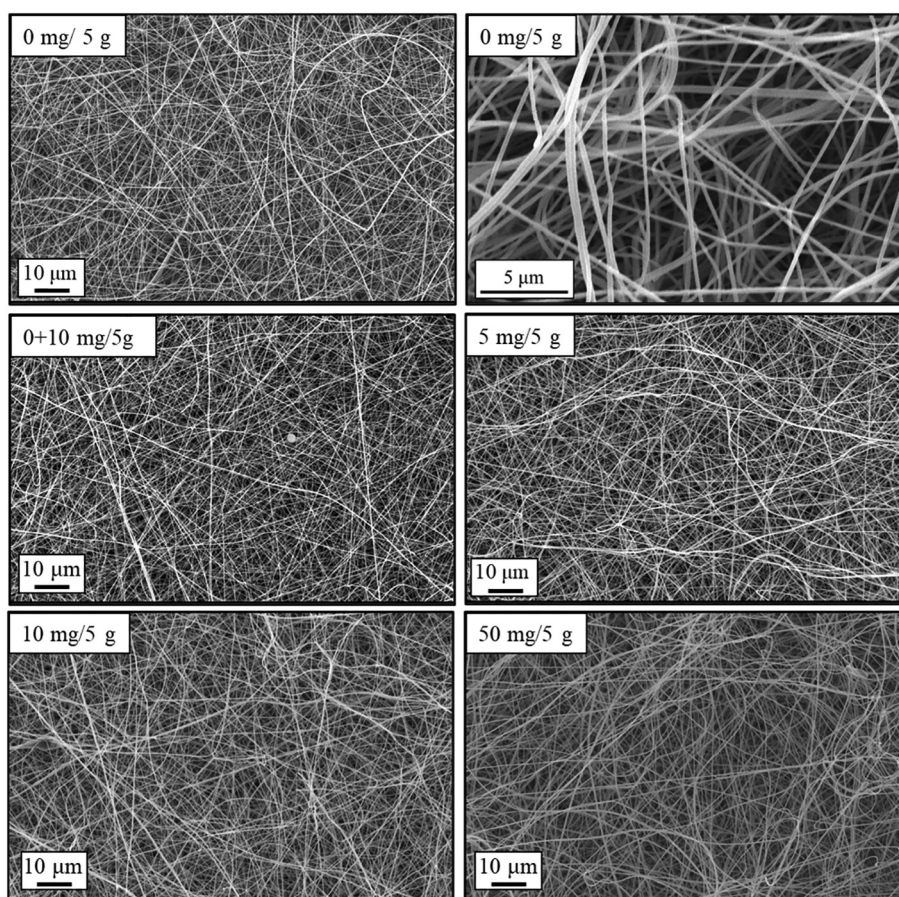


Fig. 7. SEM micrographs of AgNP/PSI and AgNP/APAP/PSI composite meshes.

Table 3
Average fibre diameter of electrospun meshes.

Paracetamol (mg/5 g)	Fibre diameter (nm)
0	210 ± 40
0 + 10	210 ± 55
5	240 ± 40
10	275 ± 75
50	325 ± 50

due to the applied voltage, and therefore the particle size measured in a colloidal state is not equivalent to the particle size within the fibres but proportional to it.

Since the nanoparticle cores are smaller than the measured size in the colloidal state, nanoparticles can easily fit inside the fibres without creating any visible deformations on the surface. Furthermore, the particle aggregates present in the 0 and 0 + 10 samples (indicated by intensity mean on Fig. 5/b) do not influence the size of the fibres since

their quantity is outweighed by smaller particles (indicated by number mean). To conclude, particle size is a key parameter which has a significant influence on the fibre diameter.

3.5. Mechanical testing and the effect of fibre diameter

To evaluate the effect of paracetamol on the mechanical parameters, tensile measurements were performed. Individual tensile curves of the meshes were very similar for every test specimen (PSI and AgNP-containing meshes with different drug concentrations as well) as it is shown in Fig. S5, Supplementary Information. The maximum value of the curves (maximum load) however is highly dependent on the thickness of the test specimen therefore maximum load in itself is not a proper value to compare the capacity of meshes of different compositions. For this purpose, a specific maximum load was calculated. The results are concluded in Fig. 9.

Since results vary in a narrow range (between 0.15 and 0.18 N*m²/g for specific maximum value in case of paracetamol containing samples),

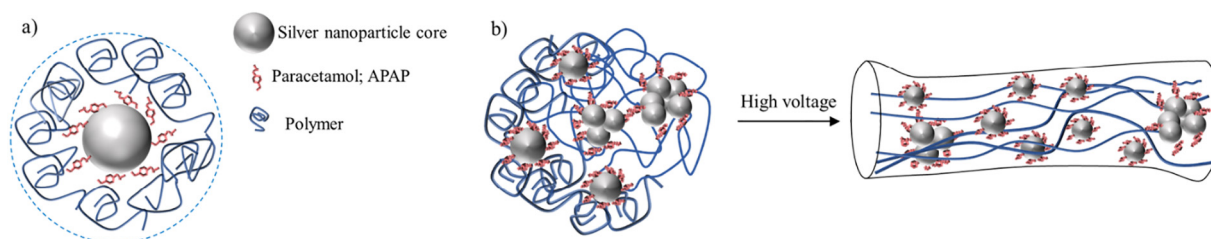


Fig. 8. a) schematic representation of particle size measured in colloidal state b) particle and fibre rearrangement during electrospinning.

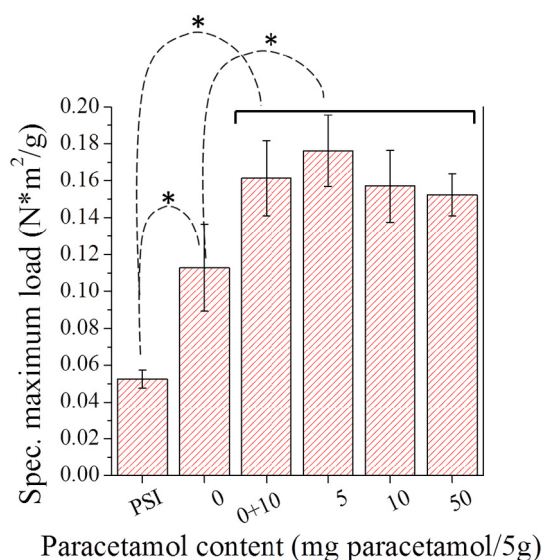


Fig. 9. Specific maximum load as a function of paracetamol content; * indicates significant difference ($p < 0.05$) between samples.

only a visual observation of the plotted graph is not sufficient to decide whether paracetamol induces a significant change in the examined property. Therefore, statistical analysis (Kruskal-Wallis test) was performed on specific maximum values as well (Table S2, Supplementary Information). Results (Fig. 9) indicate that PSI and 0 mg paracetamol/5 g samples have a significantly different mechanical capacity from every paracetamol-containing sample and from each other as well, while all paracetamol-containing samples exhibit statistically similar mechanical properties compared to each other. Based on these results, silver nanoparticles do indeed increase the specific maximum load of the meshes when compared to pure PSI membranes and interestingly the addition of paracetamol seems to further strengthen the membranes.

The underlying mechanism of the reinforcing effect of paracetamol acts on two fronts. Firstly, according to the result of fibre analysis, the presence of paracetamol in the reaction mixture alters the fibre diameter of electrospun meshes (as it was presented in the previous chapter Table 3) which can alter the mechanical properties [34]. Secondly, paracetamol may induce mild secondary bonds between polymer chains resulting in increased mechanical capacities.

To investigate the aforementioned reinforcing mechanisms, first, the correlation between fibre diameter and specific maximum load was examined.

Regarding fibre diameter, the increasing paracetamol content results in an increasing mean value except in the samples denoted as 0 + 10 mg/5 g paracetamol (Table 3). Oppositely - according to statistical analysis - the specific maximum load doesn't increase upon increasing amount of paracetamol. Specific maximum loads are approximately the same in case of every paracetamol-containing sample independently from the measured fibre diameter.

While fibre diameter is in correlation with the size of the nanoparticles, therefore, depends indirectly on paracetamol content, the specific maximum load seems to be independent on the paracetamol content in the range of 5–50 mg paracetamol/5 g: when paracetamol is present in even a small quantity (5 mg/5 g), specific maximum load increases. According to the results, the specific maximum load is also independent on the moment of paracetamol-addition (after or before the 72-hour reaction), since even in case of sample 0 + 10 mg/5 g specific maximum load is elevated compared to meshes without paracetamol.

This indicates that paracetamol doesn't alter maximum mechanical capacity through changing particle size and consequently fibre diameter, but rather through inducing weak secondary bonds.

3.6. Antibacterial properties

Silver nanoparticles are known to be effective against both Gram-positive and Gram-negative bacteria strains, however, their antibacterial spectra and properties are highly dependent on their silver-ion releasing capacity which could be hindered by the macroscopic carrier itself or even by a small-molecule drug. To evaluate whether paracetamol and/or PSI hinder or enhance the antibacterial properties of silver nanoparticles four bacteria strains were utilized. *S. epidermidis* and *P. aeruginosa* pose a high risk of wound healing as they are easily acquired and hard to eradicate with antibiotics. *B. subtilis* and *E. coli* on the other hand are frequently utilized Gram-positive and Gram-negative model strains.

PSI in itself did not prove to be effective against bacteria strains, although in some cases slightly visible, narrow clear zones around the meshes could be observed (Fig. 10/a), which might be due to PSI altering the pH locally due to its hydrolyzation [24]. The antibacterial effect of silver nanoparticles derives from silver-ion being released from the surface of nanoparticles. The efficacy against bacteria and other microorganisms is therefore dependent on the surface area: smaller nanoparticles release higher concentration of silver-ions rendering them more effective against bacteria strains [35]. Accordingly it is paramount to examine the effect of particle size on the antibacterial properties.

In addition, apart from the size of particles, shape [15] and – in our case more importantly – surface coverage also influences their antibacterial properties [36,37]. Consequently, the effect of paracetamol content can't be neglected, since increasing paracetamol content can decrease the free surface area of silver nanoparticles by increasing surface coverage. In other words, paracetamol content can have a direct effect on the antibacterial efficacy. Therefore, to visualize the effect of paracetamol on the antibacterial properties of silver nanoparticles themselves, specific antibacterial area (diffusion zone divided by silver content) was plotted as the function of composition (Fig. 10/b).

As it is indicated by the photos - showing the most and least effective compositions (Fig. 10/c and d) - and the calculated specific antibacterial area values, paracetamol content changes the antibacterial efficacy of the silver nanoparticles both in case of Gram-positive and Gram-negative bacterial strains. The antibacterial efficacy as a function of paracetamol content has a maximum value at 5 mg paracetamol/5 g PSI solution for every bacteria strain. Interestingly *S. epidermidis* seems to be more susceptible to the antibacterial effect of the synthesized system and in this case, the maximum peak is not as obvious as for the other three strains. The correlation between paracetamol content and antibacterial efficacy is not linear, therefore, it is worth to compare the particle size itself and the specific antibacterial area as well.

Fig. S6 (Supplementary Information) compares the intensity-based and the number-based particle size of the nanoparticles measured by DLS and the specific antibacterial area. Although the size measured by DLS indicates particle size in a colloidal state (Fig. 5/b) (instead of the actual size inside the mesh), a correlation can be observed between intensity-based particle size and antibacterial area. In the case of samples where intensity-based particle size (intensity mean) was large due to aggregation, the antibacterial property seems to be hindered. The two most effective samples – 5 and 10 mg paracetamol/5 g – have the lowest intensity-mean values (5 mg/5 g: 113.6 ± 1.3 nm; 10 mg/5 g: 119.9 ± 2.1 nm), indicating small particle size and low tendency for aggregation.

The number-mean size has a less obvious correlation with the antibacterial area, although, in the case of 5, 10 and 50 mg paracetamol/5 g samples, as the number mean size increases antibacterial area decreases (Fig. S6/b, Supplementary Information).

The samples with the highest paracetamol content (50 mg/5 g) didn't exhibit measurable bacterial inhibition. Since the intensity-mean size belonging to this highest paracetamol content is smaller than those of 0 and 0 + 10 samples, the lack of inhibition can be explained with the surface interaction (chemical or physical adsorption)

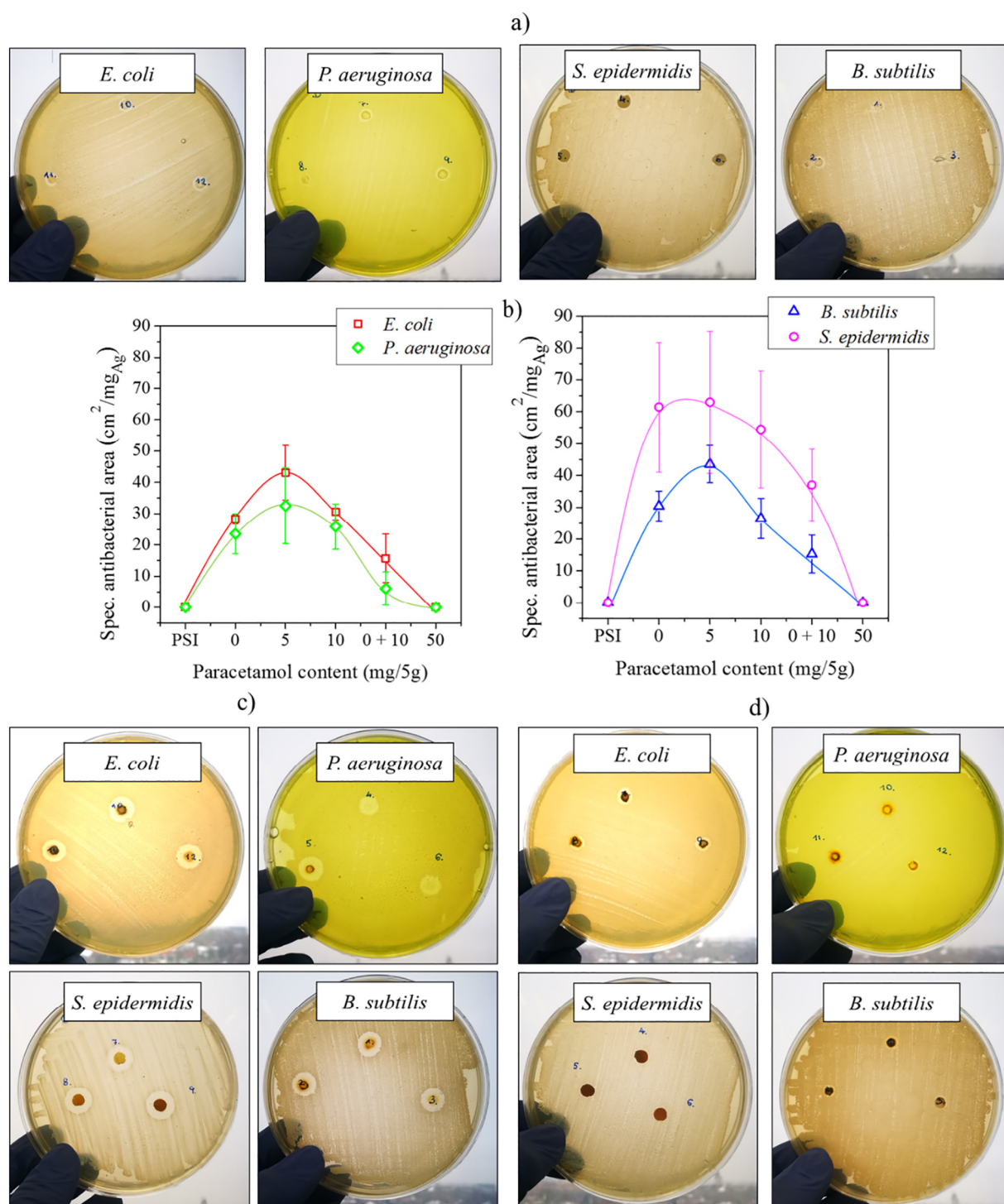


Fig. 10. a) Kirby-Bauer or Disc diffusion method using PSI membranes b) Specific antibacterial area of silver nanoparticles within electrospun meshes and diffusion zone of c) the most effective sample: 5 mg/5 g APAP meshes d) the least effective sample: 50 mg/5 g APAP meshes with all tested bacteria strains.

of silver nanoparticles and paracetamol. Small molecules can adhere to the surface of nanoparticles and therefore can affect the release of silver ions into the surrounding medium [37]. Since upon the addition of 50 mg paracetamol, antibacterial activity is completely hindered, it can be assumed that paracetamol adheres to the surface of the particles and hinders silver-ion release. The same reason can cause different specific antibacterial areas for 0 and 0 + 10 samples. While the size of the nanoparticles is the same for these two samples and therefore similar antibacterial effect would be expected, the additional paracetamol causes a slightly smaller specific antibacterial area for 0 + 10 samples.

These results highlight that the addition of a small molecule drug such as paracetamol can act in three possible ways: a. hinder the aggregation of nanoparticles which increases the surface area and therefore the antibacterial efficacy b. the increased amount of paracetamol caused an increase in the size of the nanoparticles making them less effective against bacteria c. small molecules can hinder antibacterial effect by decreasing the free surface which inhibits the silver ion release.

Results show that designing effective antibacterial nanocomposites roots in the thorough adjustment and measurement of the colloidal parameters as they have a great effect on the efficacy of the macroscopic

system. The antibacterial properties can be tuned by adjusting the size of the nanoparticles but also simply by the addition of a small molecule drug, the antibacterial efficacy could be altered.

3.7. Drug-release kinetics

For drug-release measurements two different compositions were examined, 5 and 10 mg paracetamol/5 g samples were chosen since they exhibited the highest antibacterial effect, therefore they hold promise for future applications. Drug release measurements were performed for 8 days. The kinetics could be divided into three consecutive steps with different release speed indicated by the slope of curves (Fig. 11).

In the first 1,5 h, the release occurs in a fast manner. In this period, being immersed into a physiological buffer, PSI absorbs water and an 8-fold increase in the mass of the meshes can be measured (data not shown here). Due to this water uptake and the high surface to volume ratio of the fibres a burst release of the encapsulated drug can occur (Fig. 11/a, 1st fit) [38]. In the third and second hour a slightly slower release is observed and the released amount of drug reaches approximately 40% of the encapsulated content for both composition (Fig. 11/a, 2nd fit). Subsequently, a slow release begins after 24 h (Fig. 11/b, 3rd fit). At physiological pH, PSI slowly undergoes hydrolysis and water-soluble poly(aspartic acid) is formed. During this hydrolysis, the superficial layer of the meshes starts to slowly dissolve, therefore further slow release can be observed in the following 6 days. In the case of 5 mg/5 g sample, there's a sudden increase in the released amount from 80 to 90% after 168 h. This sudden increase only occurs in the case of this smallest paracetamol content (but not in case of 10 mg/5 g paracetamol samples) indicating that increasing the paracetamol content can increase the hydrolytic stability as well. Mechanical measurements suggested that paracetamol might induce mild secondary bonds that can strengthen the membranes. These secondary bonds can have an effect on hydrolytic properties as well: higher paracetamol content can reduce the swelling capacity of meshes and increase their hydrolytic stability through the aforementioned mild secondary bonds.

Drug release studies revealed that more than 70% of the encapsulated drug can be released from electrospun PSI-AgNP nanocomposite meshes depending on the exact composition. For higher paracetamol content (10 mg/5 g) only 70% of the encapsulated drug was released, which might indicate the physical or chemical adsorption of paracetamol on the surface of silver-nanoparticles. To investigate the possible adsorption of paracetamol and reaction between the drug and silver-nanoparticles, drug-release measurements with 0 + 10 g paracetamol/5 g meshes was performed. Results are presented in Supplementary Information. Briefly, in case of physical mixture (0 + 10 mg/5 g

paracetamol) release occurred in a faster manner (Fig. S7, Supplementary Information) and based on the performed measurements the amount of release drug was also higher in case of 0 + 10 g/5 g paracetamol meshes. These data indirectly prove that during the 72-h reaction of silver nanoparticles paracetamol can adsorb chemically or physically on the surface of the nanoparticles which alters the drug-release profile of the macroscopic mesh. In case of physical mixtures, a rather sudden and fast release occurs which might be unfavourable for several medical applications. These findings were further proved by HPLC measurements performed on the release media of the aforementioned samples. The HPLC chromatograms were compared to those of pure paracetamol. Further results can be found in Supplementary Information.

4. Conclusion

In this work, we presented a one-pot synthesis method and electrospinning procedure to synthesize silver-nanoparticles with tuneable properties and subsequently fabricate polysuccinimide nanocomposite meshes with antibacterial properties. Silver nanoparticle synthesis was based on the reaction between DMF and silver-salt reported by Pastoriza-Santos et al [32,39]. Here we presented a method for the synthesis of silver nanoparticles in the presence of paracetamol and PSI at a high concentration (20 w/w%). This method results in a highly viscous polymer-nanoparticle colloidal system that is suitable for electrospinning without any further modification or addition. As it was indicated by DLS results, AgNP synthesis was successfully performed and PSI, together with paracetamol, facilitates the formation of a highly monodispersed silver colloidal system of which properties (size, aggregative stability, PDI) could be tuned by adjusting paracetamol content. A two-needle electrospinning set up proved to be successful for the effective fabrication of silver nanoparticles and paracetamol containing PSI meshes. The microstructure was observed with SEM for every composition and a correlation between particle size and fibre diameter was established. The mechanical evaluation indicated that silver nanoparticles can reinforce pure PSI membranes, and interestingly, the addition of paracetamol can further enhance the mechanical properties of the nanocomposite meshes. Antibacterial evaluation suggested that antibacterial efficacy is a function of the paracetamol content highlighting that the addition of a small molecule can change the antibacterial properties of nanoparticles which is in accordance with previous findings [36,37]. Release kinetics showed a four-stage drug release. The released amount of drug (%) was a function of exact composition as paracetamol seems to alter the hydrolytic stability of the meshes as well.

Functionalized PSI has been previously used to prepare silver-nanoparticle containing hydrogels [40], but to our knowledge, this is

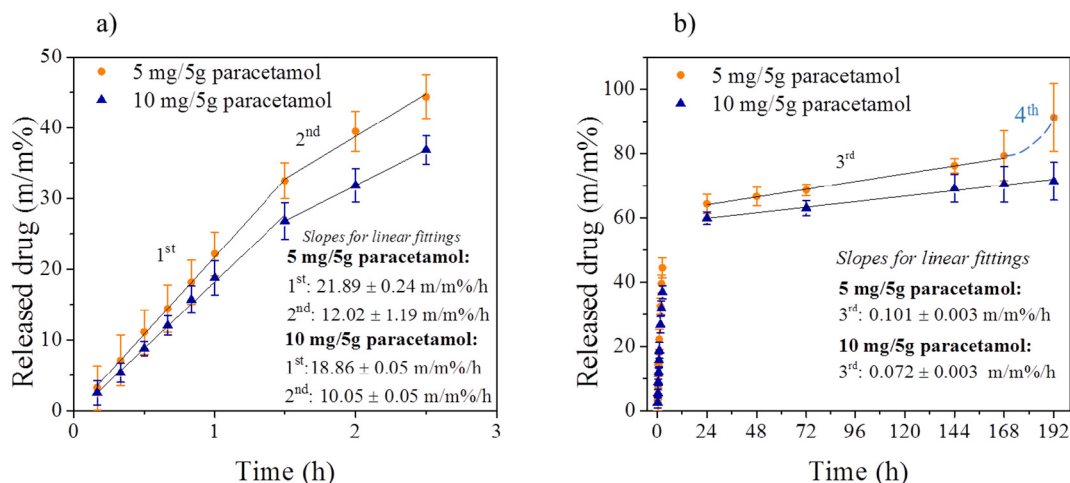


Fig. 11. Release kinetics for chosen samples: a) first 3 h, b) 7 days.

the first attempt to combine AgNP and PSI nanofibers for a drug-containing multifunctional nanocomposite. Nanoparticle containing fibrous meshes have been widely investigated [41] even using similar synthesis methods [42,43], but a comprehensive investigation both on a colloidal and macroscopic level and the comparison between nanoscale and macroscopic properties are rather rare. Additionally, this proposed synthesis and electrospinning method could be further combined with other pharmaceutical agents, moreover PSI fibres can be even combined with entirely different electrospun polymers without unwanted interactions utilizing co-electrospun technique to improve mechanical and drug-release properties [44].

CRedit authorship contribution statement

Dóra Barczikai (NP synthesis and characterization, electrospun fibre formation, SEM investigation, drug release, mechanical measurements, experiment consultant)

Viktória Kacsari (NP synthesis, drug release)

Judit Domokos (assistance in the antibacterial study)

Dóra Szabó (supervision of the antibacterial study)

Angela Jedlovsky-Hajdu (supervision of the project (original idea), preparation of the manuscript)

Declaration of competing interest

There are no known conflicts of interest associated with this publication and there has been no financial support for this work that could have influenced its outcome.

Acknowledgment

This work was supported by the National Research Development and Innovation Office (NKFIH FK 124147), the János Bolyai Research Scholarship of the Hungarian Academy of Sciences (JHA) and by the new national excellence program of the Ministry for Innovation and Technology (ÚNKP-19-4-SE-04, ÚNKP-20-5-SE-9). The research was financed by the Higher Education Institutional Excellence Programme of the Ministry for Innovation and Technology in Hungary, within the framework of the Therapeutic Development thematic programme of the Semmelweis University. 

Appendix A. Supplementary data

Supplementary data to this article can be found online at <https://doi.org/10.1016/j.molliq.2020.114575>.

References

- A.C.D.O. Gonzalez, Z.D.A. Andrade, T.F. Costa, A.R.A.P. Medrado, Wound healing - a literature review, *An. Bras. Dermatol.* 91 (2016) 614–620, <https://doi.org/10.1590/abd1806-4841.20164741>.
- A. Oliveira, S. Simões, A. Ascenso, C.P. Reis, Therapeutic advances in wound healing, *J Dermatolog Treat* 0 (2020) 000, <https://doi.org/10.1080/09546634.2020.1730296>.
- M.E. Okur, I.D. Karantas, Z. Şenyiğit, N. Üstündağ Okur, P.J. Siafaka, Recent trends on wound management: new therapeutic choices based on polymeric carriers, *Asian J Pharm Sci* (2020) <https://doi.org/10.1016/j.ajps.2019.11.008>.
- S. Dhivya, V.V. Padma, E. Santhini, Wound dressings - a review, *Biomed* 5 (2015) 24–28, <https://doi.org/10.7603/s40681-015-0022-9>.
- I. Negut, V. Grumezescu, A.M. Grumezescu, Treatment strategies for infected wounds, *Molecules* 23 (2018) 1–23, <https://doi.org/10.3390/molecules23092392>.
- U.H. Abo-Shama, H. El-Gendy, W.S. Mousa, R.A. Hamouda, W.E. Yousuf, H.F. Hetta, et al., Synergistic and antagonistic effects of metal nanoparticles in combination with antibiotics against some reference strains of pathogenic microorganisms, *Infect Drug Resist* 13 (2020) 351–362, <https://doi.org/10.2147/IDR.S234425>.
- J.O.D. Malafatti, M.P. Bernardo, F.K.V. Moreira, H. Ciol, N.M. Inada, L.H.C. Mattoso, et al., Electrospun poly(lactic acid) nanofibers loaded with silver sulfadiazine/[Mg–Al]-layered double hydroxide as an antimicrobial wound dressing, *Polym. Adv. Technol.* (2020) 1377–1387, <https://doi.org/10.1002/pat.4867>.
- K. Vowden, P. Vowden, Wound dressings: principles and practice, *Surg (United Kingdom)* 35 (2017) 489–494, <https://doi.org/10.1016/j.mpsur.2017.06.005>.
- K. Ousey, K.F. Cutting, A.A. Rogers, M.G. Rippon, The importance of hydration in wound healing: reinvigorating the clinical perspective, *J. Wound Care* 25 (2016) 122–130, <https://doi.org/10.12968/jowc.2016.25.3.122>.
- W.F. Oliveira, P.M.S. Silva, R.C.S. Silva, G.M.M. Silva, G. Machado, L.C.B.B. Coelho, et al., *Staphylococcus aureus* and *Staphylococcus epidermidis* infections on implants, *J Hosp Infect* 98 (2018) 111–117, <https://doi.org/10.1016/j.jhin.2017.11.008>.
- J. Stewart, A short note on the nutritive value of linseed cake, *J. Agric. Sci.* 18 (1928) 702–703, <https://doi.org/10.1017/S002185960009278>.
- L. Wang, C. Hu, L. Shao, The antimicrobial activity of nanoparticles: present situation and prospects for the future, *Int. J. Nanomedicine* 12 (2017) 1227–1249, <https://doi.org/10.2147/IJN.S121956>.
- Z. Pang, R. Raudonis, B.R. Glick, T.J. Lin, Z. Cheng, Antibiotic resistance in *Pseudomonas aeruginosa*: mechanisms and alternative therapeutic strategies, *Biotechnol. Adv.* 37 (2019) 177–192, <https://doi.org/10.1016/j.biotechadv.2018.11.013>.
- A. Elbourne, R.J. Crawford, E.P. Ivanova, Nano-structured antimicrobial surfaces: from nature to synthetic analogues, *J. Colloid Interface Sci.* 508 (2017) 603–616, <https://doi.org/10.1016/j.jcis.2017.07.021>.
- N.Y. Lee, W.C. Ko, P.R. Hsueh, Nanoparticles in the treatment of infections caused by multidrug-resistant organisms, *Front. Pharmacol.* 10 (2019) 1–10, <https://doi.org/10.3389/fphar.2019.01153>.
- I. Khansa, A.R. Schoenbrunner, C.T. Kraft, J.E. Janis, Silver in wound care - friend or foe?: a comprehensive review, *Plast Reconstr Surg - Glob Open* 7 (2019) 1–10, <https://doi.org/10.1097/GOX.0000000000002390>.
- S.M. Dizaj, F. Lotfipour, M. Barzegar-Jalali, M.H. Zarrintan, K. Adibkia, Antimicrobial activity of the metals and metal oxide nanoparticles, *Mater Sci Eng C* 44 (2014) 278–284, <https://doi.org/10.1016/j.msec.2014.08.031>.
- E. Zdraveva, J. Fang, B. Mijovic, T. Lin, Electrospun Nanofibers, 2016 <https://doi.org/10.1016/B978-0-08-100550-7.00011-5>.
- R. Rošic, P. Kocbek, J. Pelipenko, J. Kristl, S. Baumgartner, Nanofibers and their biomedical use, *Acta Pharma.* 63 (2013) 295–304, <https://doi.org/10.2478/acph-2013-0024>.
- I. Sebe, E. Ostorhazi, A. Fekete, K.N. Kovacs, R. Zelko, I. Kovalszky, et al., Polyvinyl alcohol nanofiber formulation of the designer antimicrobial peptide APO sterilizes *Acinetobacter baumannii*-infected skin wounds in mice, *Amino Acids* 48 (2016) 203–211, <https://doi.org/10.1007/s00726-015-2080-4>.
- A.R. Unnithan, N.A.M. Barakat, P.B. Tirupathi Pichiah, G. Gnanasekaran, R. Nirmala, Y.S. Cha, et al., Wound-dressing materials with antibacterial activity from electrospun polyurethane-dextran nanofiber mats containing ciprofloxacin HCl, *Carbohydr. Polym.* 90 (2012) 1786–1793, <https://doi.org/10.1016/j.carbpol.2012.07.071>.
- H. Maleki, S. Mathur, A. Klein, Antibacterial Ag containing core-shell polyvinyl alcohol-poly (lactic acid) nanofibers for biomedical applications, *Polym. Eng. Sci.* (2020) 1–10, <https://doi.org/10.1002/pen.25375>.
- P. Zahedi, I. Rezaeian, S.O. Ranaei-Siadat, S.H. Jafari, P. Supaphol, A review on wound dressings with an emphasis on electrospun nanofibrous polymeric bandages, *Polym. Adv. Technol.* 21 (2010) 77–95, <https://doi.org/10.1002/pat.1625>.
- E. Krisch, B. Gyarmati, D. Barczikai, V. Lapeyre, B.A. Szilágyi, V. Ravaine, et al., Poly (aspartic acid) hydrogels showing reversible volume change upon redox stimulus, *Eur. Polym. J.* 105 (2018) 459–468, <https://doi.org/10.1016/j.eurpolymj.2018.06.011>.
- K. Molnar, A. Jedlovsky-Hajdu, M. Zrinyi, S. Jiang, S. Agarwal, Poly(amino acid)-based gel fibers with pH responsivity by coaxial reactive electrospinning, *Macromol. Rapid Commun.* 38 (2017) 1–5, <https://doi.org/10.1002/marc.201700147>.
- P. Ferruti, S. Manzoni, S.C.W. Richardson, R. Duncan, N.G. Patrik, R. Mendichi, et al., Amphoteric linear poly(amido-amine)s as endosomolytic polymers: correlation between physicochemical and biological properties, *Macromolecules* 33 (2000) 7793–7800, <https://doi.org/10.1021/ma000378h>.
- S. Km, J.-H. Kim, D. Kim, pH sensitive swelling and releasing behavior of nano-gels based on polyaspartamide graft copolymers, *J. Colloid Interface Sci.* 356 (2011) 100–106.
- J. Liu, C. Jin, C. Wang, Hyperbranched thiourea-grafted electrospun polyacrylonitrile fibers for efficient and selective gold recovery, *J. Colloid Interface Sci.* 561 (2020) 449–458.
- G. Piccirillo, B. Bochicchio, A. Pepe, K. Schenke-Layland, S. Hinderer, Electrospun poly-L-lactide scaffold for the controlled and targeted delivery of a synthetically obtained diclofenac prodrug to treat actinic keratosis, *Acta Biomater.* 52 (2017) 187–196.
- S. Homaeigozar, A.R. Boccaccini, Antibacterial biohybrid nanofibers for wound dressings, *Acta Biomater.* 107 (2020) 25–49, <https://doi.org/10.1016/j.actbio.2020.02.022>.
- K. Molnar, D. Juriga, P.M. Nagy, K. Sinko, A. Jedlovsky-Hajdu, M. Zrinyi, Electrospun poly(aspartic acid) gel scaffolds for artificial extracellular matrix, *Polym. Int.* 63 (2014) 1608–1615, <https://doi.org/10.1002/pi.4720>.
- I. Pastoriza-Santos, L.M. Liz-Marzán, Formation of PVP-protected metal nanoparticles in DMF, *Langmuir* 18 (2002) 2888–2894, <https://doi.org/10.1021/la015578g>.
- S. Bhattacherjee, Review article DLS and zeta potential – what they are and what they are not? *J. Control. Release* 235 (2016) 337–351, <https://doi.org/10.1016/j.jconrel.2016.06.017>.
- A. Baji, Y.-W. Mai, S.-C. Wong, Effect of fiber size on structural and tensile properties of electrospun polyvinylidene fluoride fibers, *Polym. Eng. Sci.* 2 (2015) <https://doi.org/10.1002/pen>.
- Y. Qing, L. Cheng, R. Li, G. Liu, Y. Zhang, X. Tang, et al., Potential antibacterial mechanism of silver nanoparticles and the optimization of orthopedic implants by advanced modification technologies, *Int. J. Nanomedicine* 13 (2018) 3311–3327, <https://doi.org/10.2147/IJN.S165125>.

- [36] Jingyu, David A. Sonshine, R.H.H. Saira Shervani, Controlled release of biologically active silver from nanosilver surfaces, *ACS Nano* 4 (2010) 6903–6913, <https://doi.org/10.1021/nn102272n>.
- [37] Y.M. Long, L.G. Hu, X.T. Yan, X.C. Zhao, Q.F. Zhou, Y. Cai, et al., Surface ligand controls silver ion release of nanosilver and its antibacterial activity against *Escherichia coli*, *Int. J. Nanomedicine* 12 (2017) 3193–3206, <https://doi.org/10.2147/IJN.S132327>.
- [38] Y.J. Son, W.J. Kim, H.S. Yoo, Therapeutic applications of electrospun nanofibers for drug delivery systems, *Arch. Pharm. Res.* 37 (2014) 69–78, <https://doi.org/10.1007/s12272-013-0284-2>.
- [39] I. Pastorizo-Santos, L.M. Liz-Marzán, N,N-dimethylformamide as a reaction medium for metal nanoparticle synthesis, *Adv. Funct. Mater.* 19 (2009) 679–688, <https://doi.org/10.1002/adfm.200801566>.
- [40] M. Tan, Y. Choi, J. Kim, J.H. Kim, K.M. Fromm, Polyaspartamide functionalized catechol-based hydrogels embedded with silver nanoparticles for antimicrobial properties, *Polymers (Basel)* 10 (2018) <https://doi.org/10.3390/polym10111188>.
- [41] C.L. Zhang, S.H. Yu, Nanoparticles meet electrospinning: recent advances and future prospects, *Chem. Soc. Rev.* 43 (2014) 4423–4448, <https://doi.org/10.1039/c3cs60426h>.
- [42] H.K. Lee, E.H. Jeong, C.K. Baek, J.H. Youk, One-step preparation of ultrafine poly(acrylonitrile) fibers containing silver nanoparticles, *Mater. Lett.* 59 (2005) 2977–2980, <https://doi.org/10.1016/j.matlet.2005.05.005>.
- [43] A.K. Selvam, G. Nallathambi, Polyacrylonitrile/silver nanoparticle electrospun nanocomposite matrix for bacterial filtration, *Fibers Polym* 16 (2015) 1327–1335, <https://doi.org/10.1007/s12221-015-1327-8>.
- [44] C. Voniatis, L. Balsevicius, D. Barczikai, D. Juriga, A. Takács, L. Kóhidai, et al., Co-electrospun polysuccinimide/poly(vinyl alcohol) composite meshes for tissue engineering, *J. Mol. Liq.* 306 (2020) <https://doi.org/10.1016/j.molliq.2020.112895>.